Dissecting Dynamics near the Glass Transition

*Khalil Akkaoui, Joseph B. Schlenoff**

Department of Chemistry and Biochemistry

The Florida State University, Tallahassee, FL 32306 USA

Abstract

Though the strong transformation in mechanical properties of glass-forming materials near the glass transition, T_g, has been recognized and exploited for millenia, efforts to understand and predict this phenomenon at a molecular level continue to this day. Close to T_g, where relaxation is considerably slower than predicted by the well-known Arrhenius equation, one of the most versatile and widely-used expressions to describe the dynamics or relaxation of glass formers is that of Vogel, Fulcher and Tammann (VFT). The VFT equation, introduced nearly 100 years ago, contains three adjustable fit parameters. In this work the dynamics of the polymer repeat units are related to macroscopic dynamics in polyelectrolyte complexes, which are hydrated amorphous blends of charged polymers. A simple expression, containing no freely adjustable fit parameters, is derived to quantitatively model relaxation from T_g to temperatures well into the Arrhenius region. The new expression, which also fits a selection of three common neutral polymers, will advance the understanding and use of the glass-forming phenomenon.

*jschlenoff@fsu.edu

Introduction

The mechanical relaxation rate of a glass-forming material,[1] such as a polymer in a melt or rubbery state, follows the well-known Arrhenius relationship at sufficiently high temperatures

$$\omega_{T,arr} = \omega_0 e^{\frac{-E_{act}}{RT}} \qquad [1]$$

where $\omega_{T,arr}$ is the relaxation rate, ω_0 is a prefactor and E_{act} an activation energy.[2] Such a dependence reflects well-localized dynamics with minimal cooperativity beyond a short length scale. On further cooling, the relaxation rate decreases faster than predicted by Equation 1 to, and past, the glass transition temperature, T_g, whereupon the material has reached a glassy state with significantly higher modulus. Figure 1 illustrates the temperature dependence of the relaxation rate (frequency) of a typical amorphous polymer using a classical set of lnω versus 1/T coordinates.

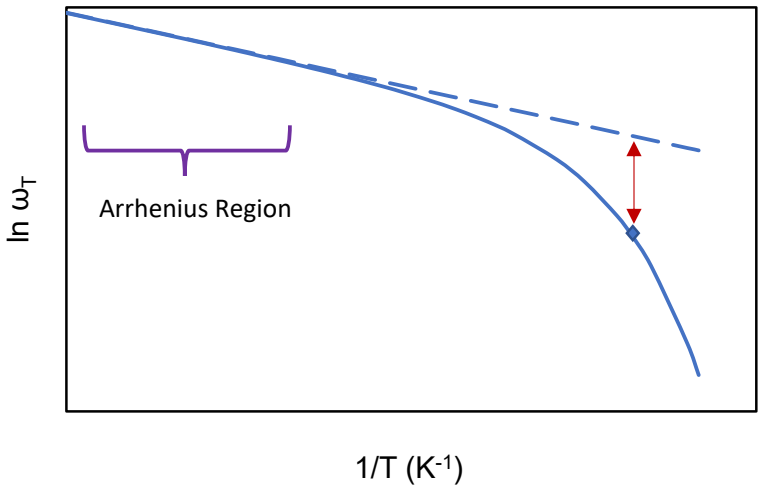

Figure 1. Sketch of relaxation rate, ω_T, as a function of temperature for a typical glass former. At higher temperatures (towards the left) relaxation typically slows on cooling according to the Arrhenius behavior ($\omega_T \sim e^{-1/T}$) until about 100 K above T_g (T_g shown at the

diamond) whereupon the decrease in relaxation rate accelerates (deviation from Arrhenius indicated by arrow).

A quantitative description of the glass transition using physically relevant and measurable parameters remains one of the greatest challenges in science.[3,4] Over the past several decades, many significant advances have been made in understanding the microscopic mechanisms of the glass transition. However, the frequency response of polymers as a function of temperature is still modeled or fit by a handful of equations which contain semiempirical fit parameters. The best-known fits that focus on the non-Arrhenius region near T_g are the Vogel-Fulcher-Tammann, VFT, with origins nearly a century old,[5-7] and Williams–Landel–Ferry, WLF,[8] equations, which are mathematically equivalent but highlight different aspects of polymer dynamics. The VFT fit includes a high frequency prefactor, $\omega_{0,VFT,}$ commonly about 1×10^{10} s^{-1}, and two additional fit parameters, D and T_o (Equation 2).

$$\omega_{T,VFT} = \omega_{o,VFT}\, e^{\frac{-DT_o}{T-T_o}} \qquad [2]$$

The temperature T_o, known as the Vogel temperature, implies divergent properties ($\omega = 0$ at T_o) of the relaxation time[9] and has initiated vigorous debate over whether polymers continue to flow or relax below T_o,[10,11,12] invoking flow from materials > 10^7 years old.[13] The WLF fit, Equation 3, shifts data from frequencies measured at temperature T to a reference temperature T_r using a shift factor a_T and focuses on constants C_1 and C_2 and whether they become "universal" if the reference temperature is selected to be T_g.

$$\log a_T = \frac{C_1(T-T_r)}{C_2+T-T_r} \qquad [3]$$

The dynamics of chains rely on the dynamics of the repeat, or monomer, units from which they are made. Thus, quantitative expressions for chain dynamics require understanding the dependence of repeat unit dynamics on temperature. The idea of a cooperatively rearranging region, CRR, discussed at length by Adam and Gibbs,[9] is often used to understand

the molecular level picture of processes approaching T_g: the number of cooperatively rearranging units, CRUs, involved in the CRR is a minimum and remains constant in the Arrhenius region. As the polymer is cooled, this number grows[14] approaching T_g and the energy required to activate the growing CRR increases accordingly, pressing the slope in Figure 1 downwards.

In a recent study of ion transport in polyelectrolyte complexes - stoichiometric blends of oppositely-charged polymers - it was found that the rate of ion diffusion through the polymer was an excellent reporter of repeat unit dynamics.[15] Polyelectrolyte complexes, PECs, also termed coacervates when in a more liquidlike form,[16] phase separate on mixing aqueous solutions of oppositely-charged polymers Pol_N^+ and Pol_N^-

$$(Pol^+A^-)_{N,aq} + (Pol^-M^+)_{N,aq} \rightarrow (Pol^+Pol^-)_N + NA^-_{aq} + NM^+_{aq} \qquad [4]$$

The driving force for this association stems mainly from the release of counterions M^+ and A^- into solution, moderated by small enthalpy changes. The PEC may be "doped" with small "salt" ions, partially reversing Equation 4,[17] providing an ion-transporter with variable, high conductivity.[18]

As with most ion-conducting polymers, the dynamics of ion hopping depend on the dynamics of the charged repeat units Pol^+ or Pol^-. Prior work on a PEC at temperatures well above the T_g, i.e. in the Arrhenius region, showed that repeat unit relaxation times could be directly correlated with ion hopping, which was given by the ionic conductivity.[15,18] The entangled polyelectrolytes showed an unusual scaling of viscosity, η, as a function of number of repeat units N: $\eta \sim N^5$. Using a theory of "sticky" reptation,[19] polymer chain dynamics were connected to those of the repeat unit[15] to obtain a quantitative relationship of η versus N.

In the present work, two PECs, both with a T_g near room temperature, were used to explore the relationship between repeat unit and polymer dynamics, and temperature: one was made from poly(diallyldimethylammonium), PDADMA, and poly(styrene sulfonate), PSS; the

second from poly(vinylbenzyltrimethylammonium), PVBT, and poly(acrylamidomethyl propanesulfonate) PAMPS. PEC properties were always measured with an equilibrium content of water, maintained by contact with aqueous solutions, which provides reproducible properties and glass transitions near room temperature. Because the activation energy for rearrangement of $Pol^{+}Pol^{-}$ monomer pairs can be measured, the temperature dependence of the PEC near T_g can be rationalized in terms of a *specific* number of cooperatively rearranging pairs. This leads to a simple expression, containing no freely adjustable fit parameters, for the relaxation of PECs to and through the glass transition. Extension to a selection of common neutral polymers illustrates the breadth of validity for the new expression.

Results and Discussion

Compact PECs were prepared using pairs of oppositely-charged polyelectrolytes, one with a narrow molecular weight distribution, Đ, and one with a broad Đ. To obtain the relaxation behavior of polymer segments, ionic conductivity was first measured as a function of temperature. Using the Nernst Einstein equation, conductivities were converted to diffusion coefficients.[15] Diffusion was modeled using a simple nearest-neighbor hopping mechanism to obtain the relaxation rate, including the activation energy, of a $Pol^{+}Pol^{-}$ charge pair. PEC studies as a function of temperature were limited to the range 0 – 90 ºC because of the aqueous baths in which they were immersed. Hydrated PDADMA/PSS has a glass transition temperature near 30 ºC whereas PVBT/PAMPS has a T_g just above 0 ºC (see Supporting Information Figures S1, S2 and S3).

Monomer Dynamics

The 4-probe conductivity method described in Experimental provided an accurate and reproducible measure of conductivity *versus* temperature for PDADMA/PSS and PVBT/PAMPS PECs doped with NaCl to a low level. At the solution salt concentration employed, 0.10 M, the NaCl concentrations inside PDADMA/PSS and PVBT/PAMPS were 0.0443 M and 0.0624 M, respectively. The conductivity, σ (Ω^{-1} cm^{-1}), was converted to the ion diffusion coefficient, D_i (cm^2 s^{-1}), at temperature T using the Nernst-Einstein equation

$$\sigma = \frac{2q^2 C D_i N_a}{kT} \qquad [5]$$

where q is the charge of one ion (1.602 x 10^{-19} C), C is the concentration of NaCl inside the PEC, N_a is Avogadro's number, and k is Boltzmann's constant. D_i shows Arrhenius behavior as a function of temperature (see Figure 2).

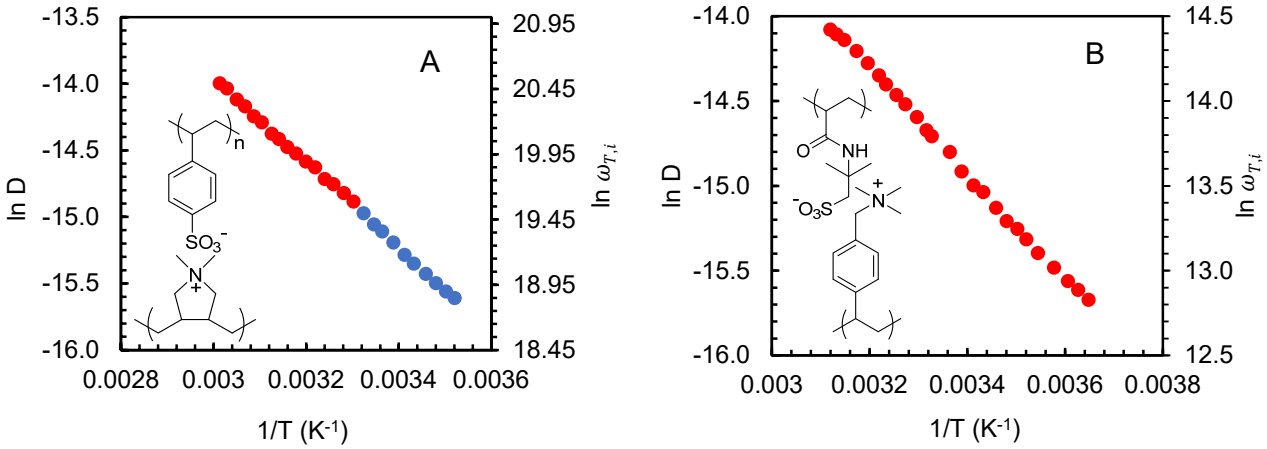

Figure 2. Arrhenius plot of the diffusion coefficient, left axis (in cm^2 s^{-1}) and ion hopping rate (right axis in s^{-1}), as a function of 1/T for ion transport in PDADMA/PSS (Panel A) and PVBT/PAMPS (Panel B), both doped in 0.1 M NaCl. For PDADMA/PSS, the slope, with a slight change near T_g = 30 °C, provides activation energies, E_a, of 25.6 kJ mol^{-1} above

T_g and 27.1 kJ mol^{-1} below T_g. For PVBT/PAMPS the activation energy above T_g = 0 °C was 25.9 kJ mol^{-1}. Insets show structures.

An interesting feature of the ion diffusion plot for PDADMA/PSS in Figure 2A is the slight but clear break in slope at about 30 ºC, near the glass transition temperature measured from dynamic mechanical analysis. At temperatures above 30 ºC the activation energy, E_a, is 25.6 kJ mol^{-1} and below it is 27.1 kJ mol^{-1}. Similar results were obtained for PDADMA/PSS PEC doped with 0.3 M NaCl.[18]

The PVBT/PAMPS PEC, with a T_g of 0 °C allowed the maximum temperature range above T_g. Na^+ and Cl^- salt ions are decoupled when they enter a PEC, and disperse to maximize their entropy but remain associated with Pol^+ or Pol^- repeat units as counterions.[15]

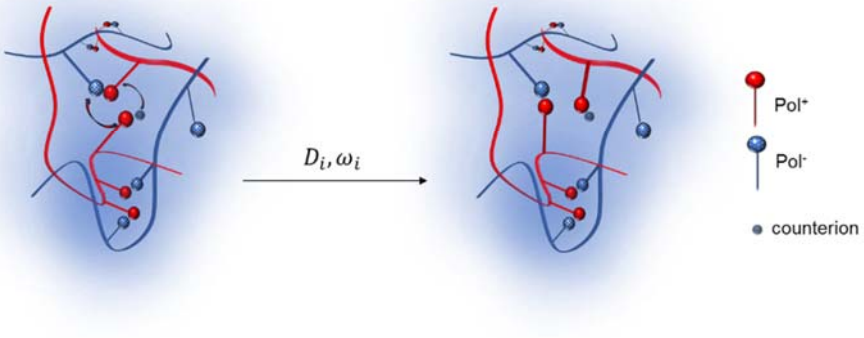

Scheme 1. Hopping of a chloride ion in complexed positive, Pol^+, and negative, Pol^-, polyelectrolyte. The hopping step relies on breaking of a neighboring Pol^+Pol^- pair. The activation energy is $E_{a,u}$. Only the centers of mass for the polymer backbones (lines) and pendant functional groups (spheres) are shown to more clearly illustrate the pairing and exchange.

Scheme 1 depicts one ion hopping event for a Cl^- ion as it switches places to occupy an adjacent Pol^+ counterion site. Hopping is controlled by the dynamics of neighboring Pol^+Pol^- pairs: hopping is only allowed if the destination Pol^+Pol^- pair is open. The ion diffusion coefficient is modeled in 3-dimensions by a nearest-neighbor hopping distance d and a temperature-dependent ion hopping rate $\omega_{T,i}$

$$D_i = \frac{\omega_{T,i} d^2}{6} \qquad [6]$$

The hopping distance is the average separation between polymer pairs, which is 0.79 nm for this PDADMA/PSS and 0.92 nm for PVBT/PAMS. The hopping rate expression follows Arrhenius behavior

$$\omega_{T,i} = \omega_{0,i} e^{\frac{-E_a}{RT}} = \omega_{0,i} p_T \qquad [7]$$

The prefactor $\omega_{0,i}$, here 8.12 x 10^{12} s^{-1}, represents the hopping attempt frequency and the exponential term can be considered the probability, p_T, that a hopping attempt will be successful at a particular temperature. It is also clear from Scheme 1 that the ion hopping rate is the same as the rate of Pol^+Pol^- pair breaking frequency, and Equation 7 directly provides the temperature dependence for this process which is fundamental to longer-range dynamics.

The Minimum Cooperative Rearranging Region (MCRR)

Cooperative rearrangement is the coordinated movement of a certain number of "units," such as chain segments, in a certain volume known as the cooperatively rearranging region.[9] Though the minimum number of units moving cooperatively is understood to be two, the *identity* of the units and *how* they move has historically been unclear.[9] Here, the most likely mode of rearrangement in PECs ensures ion pairing is preserved to minimize the electrostatic

energy. To accomplish this, pair exchange, PE, was proposed.[20] In the PE mechanism, two neighboring Pol^+Pol^- pairs exchange places, as illustrated in Scheme 2

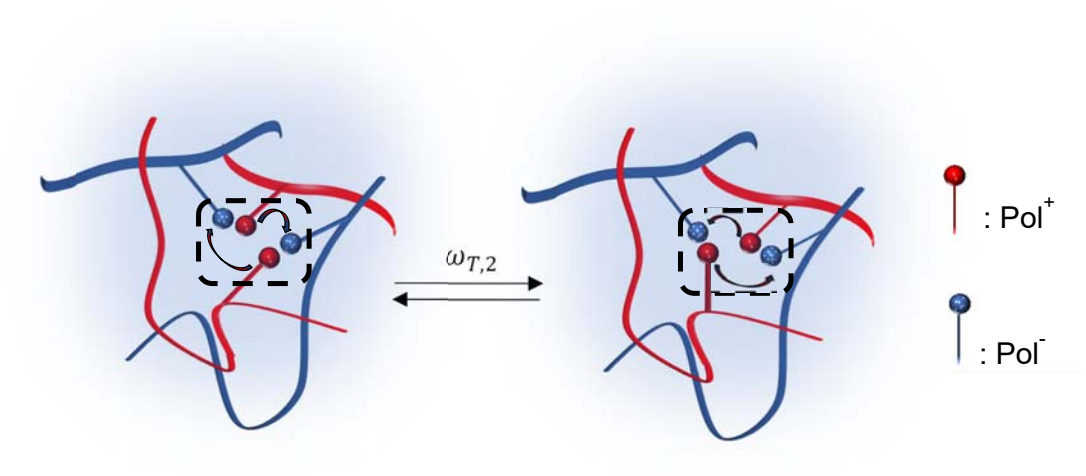

Scheme 2. The minimum cooperative rearranging unit in a polyelectrolyte complex. Two Pol^+Pol^- pairs exchange places at a rate $\omega_{T,2}$ or $\omega_{T,arr}$. The activation energy is $2E_{a,u}$.

Pair exchange allows polymer chains to move relative to each other. The displacement is minimal and the net energy is similar before and after exchange because all four charged units are paired before and after the event.

The MCRR is a thus two Pol^+Pol^- pairs, or a quad of charged units. In the Arrhenius region of viscoelastic response, PE is the only relaxation mechanism in operation, i.e. there is no cooperativity beyond exchanging quads. Recently, the mechanical properties of a more fluid-like PEC, PMAPTA/PMA, were studied at temperatures well above its T_g.[15] The viscoelastic properties followed an Arrhenius response with temperature. Importantly, the activation energy could be predicted knowing the (experimentally measured) activation energy for ion hopping, $E_{a,u}$, for breaking one pair (Scheme 1): the activation energy corresponding to the simultaneous breaking of two pairs in Scheme 2 was simply $2E_{a,u}$.[15]

Relaxation and Deviation from Arrhenius

To understand the dramatic slowing of dynamics approaching the glass transition, the degree of cooperativity[9] may be dissected down to the number of units, *n*, rearranging cooperatively at any temperature. If the activation energy for each unit is $E_{a,u}$, the activation energy for *n* cooperatively rearranging units is $nE_{a,u}$ and the relaxation rate at that temperature $\omega_{T,n}$ is

$$\omega_{T,n} = \omega_{o,n}\, e^{-\frac{nE_{a,u}}{RT}} \qquad [8]$$

The slope of the line of a plot of $\ln\omega_{T,n}$ at any 1/T is $-nE_{a,u}/R$. i.e.

$$\frac{d}{d}\frac{ln\omega_{T,n}}{T^{-1}} = -\frac{nE_{a,u}}{R} \qquad [9]$$

For the Arrhenius region, $n = 2$

$$\omega_{T,Arr} = \omega_{o,A} e^{-\frac{2E_{a,u}}{RT}} \qquad [10]$$

The deviation of $\ln\omega_{T,n}$ from Arrhenius as $T \rightarrow T_g$ is modeled using some key concepts employed by Adam and Gibbs in their seminal paper on the CRR.[9] They expressed the relaxation rate in glass formers as a transition probability, W

$$W = Ae^{-z\Delta\mu/kT} \qquad [11]$$

where A is a temperature independent prefactor, z is the number of monomer units (the "size") in the cooperative region, and Δμ is the energy barrier for rearrangement per monomer segment. Although the identity of the monomer unit is implied to be a segment, this was not specified and has, to date, been left open for interpretation. Equating z to n and Δμ to $E_{a,u}$ the relative relaxation rates in the Arrhenius region (n = 2) and any other temperature is given by

$$ln\left(\frac{\omega_{T,arr}}{\omega_{T,n}}\right) = n - 2 \qquad [12]$$

On a log plot, $\omega_{T,n}$ shows clearly as a deviation from Arrhenius, illustrated in Figure 1. Similar conclusions can made starting from molecular entropy theories,[21,22] which are extensions of ideas presented by Adam and Gibbs.

Using Equations 9 and 12 along with the following boundary condition from $n = 3$ for Equation 12:

$$\omega_{T,3} = \frac{\omega_{T,arr}}{e} \qquad [13]$$

an equation for $\omega_{T,n}$ at any temperature may be derived (see Supporting Information for the derivation):

$$ln\omega_{T,n} = ln\omega_{T,arr} - e^{\frac{E_{a,u}}{R}\left(\frac{1}{T}-\frac{1}{T_c}\right)} \qquad [14]$$

where T_c is the convergence temperature, defined at the point where $\omega_{T,n}$ converges to a factor of 1/e of the Arrhenius value, which occurs at $n = 3$ (Equation 13). There are other ways to present Equation 14, but this form emphasizes the extent of deviation (second term on the right)

from Arrhenius. Figure 3 compares the data to Equation 14.

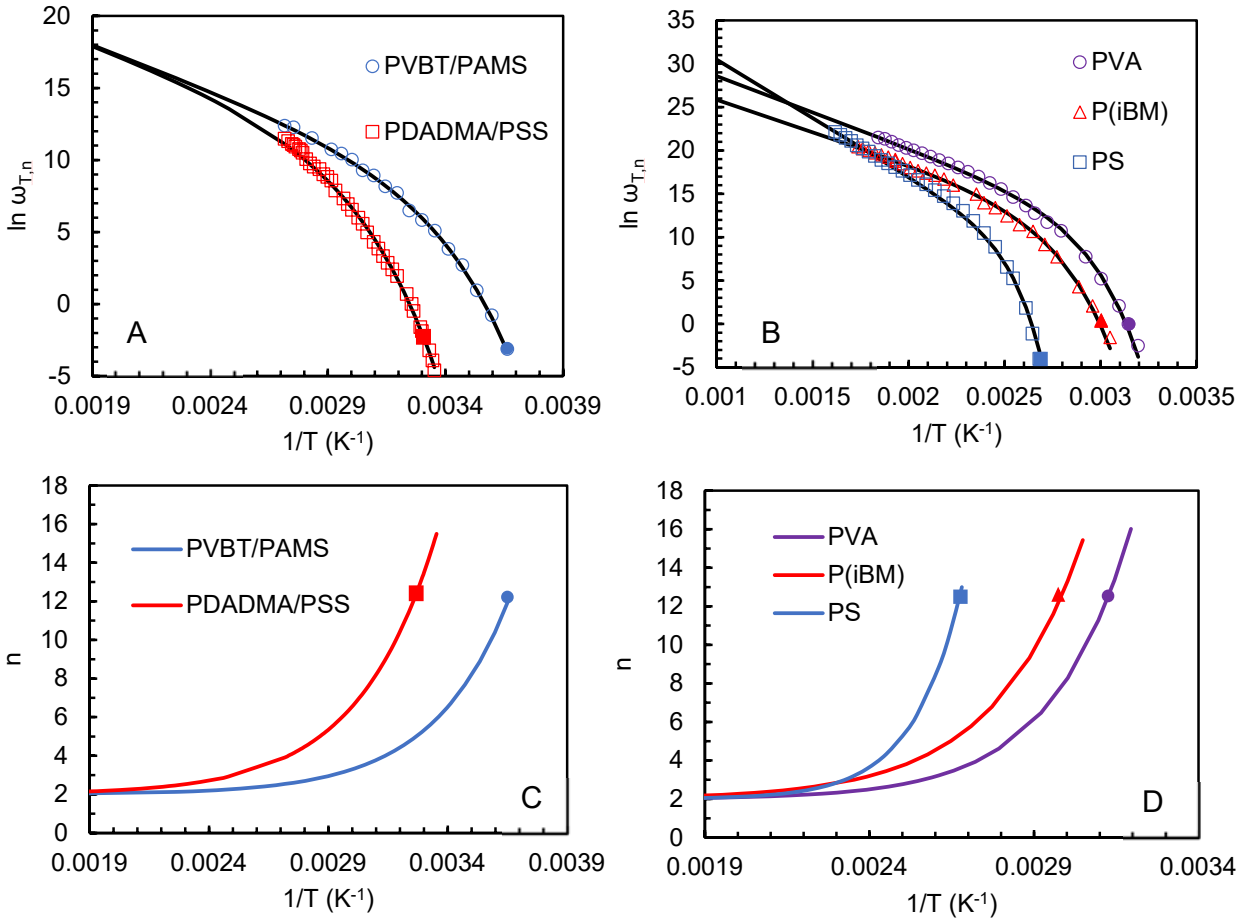

Figure 3. **A. PEC relaxation rate as a function of 1/T for the PECs PDADMA/PSS and PVBT/PAMPS. B. Relaxation rate of neutral polymers PVA, PiBM and PS well into the Arrhenius region**. Open markers represent the experimental relaxation frequency with the closed marker denoting T_g. The solid lines are plots of Equation 14 using the parameters $E_{a,u}$ and T_c listed in Table 1. Panels **C** and **D** present the number of rearranging units in the CRR as a function of temperature for the PECs and neutral polymers respectively with $n \sim 13$ at T_g and $n = 2$ in the Arrhenius region at high temperatures.

Table 1. Parameters used/deduced for Equation 14 for the relaxation behavior in Figure 3 and for comparison VFT fits. Neutral polymers in columns 2-4, PECs in columns 5 & 6.

	PS	PVA	P(iBM)	PVBT/PAMPS	PDADMA/PSS
$E_{a,u}$ (kJ mol^{-1})	56.1	34.8	31	25.9	25.6
$\omega_{o,A}$ (s^{-1})	1.27 x 10^{19}	1.14x10^{16}	3.12x10^{14}	9.51x10^{12}	8.15x10^{12}
T_g (K)	373	313	328	273	303
T_c (K)	430	390	425	343	399
T_c/T_g	1.15	1.25	1.26	1.26	1.31
n_{Tg} (±1)	13.4	13.4	13.3	13.1	13.7
D_{VFT}	4.2	5.3	5.4	5.4	5.8
$\omega_{o,VFT}$ (s^{-1})	6.0x10^{10}	1.0x10^{11}	5.0x10^{10}	1.0x10^{9}	1.2x10^{10}
T_0 (K)	324	263	271	222	250
m_{VFT}	105	75.8	64.5	54.6	63.2
m	103	75.6	64.1	64.6	57.3
U (J mol^{-1} K^{-1})	19.9	21.9	21.6	19.4	20.2

Neutral Polymers

While the PEC data are predicted well by Equation 14, the upper limit of temperature for these samples is set by the boiling point of water (i.e. ca 100 ºC), and it was not possible to scan up to the 100 degrees or so above T_g to reach the Arrhenius region. Instead, the Arrhenius activation energy (two Pol^+Pol^- pairs in the CRR) was obtained simply by doubling the activation energy for one pair.

Such an exercise is not possible for neutral polymers, since there are no ions to report the hopping (pair breaking) rate in Equation 6. However, the logic pertaining to the number and increase in CRUs should apply to neutral polymers and the upper limits of accessible temperature are considerably higher. Three common neutral polymers, polystyrene, polyvinylacetate and poly(isobutylmethacrylate), were obtained from commercial sources and used without further purification. All three had molecular weights above 10^5, selected to minimize the dependence of T_g on molecular weight, and broad Đ of about 2. The linear viscoelasticity of the neutral polymers was evaluated from T_g to well into the Arrhenius region

(Figure 3, see Supporting Information Figure S4 for shift factors). The activation energies from the Arrhenius slope (= $2E_{a,u}$), T_g and T_c for all the polymers studied are summarized in Table 1. As seen in Figure 3, Equation 14 was exceptional in describing the dynamics of the three neutral polymers as well.

T_c is between 60 and 100 degrees above T_g, comparable with the general statement that Arrhenius behavior is observed beyond T_g + 100. Partly in response to the controversy surrounding T_o, a characteristic temperature, T_x, for a transition from VFT to Arrhenius dependence has been sought in various analyses.[23] The crossover from VFT to Arrhenius depends on what is plotted. For example, a plot of $\log\omega_T$ versus $1/T-T_o$ yields a T_x (also labeled an "onset" temperature[24,25]) close to T_c seen here,[23] whereas a power law fit returns a lower T_x more aligned with mode coupling theory.[26,27]

Comparison with VFT

There are several significant aspects to Equation 14 in comparison to the VFT Equation, which also does a good job of fitting the data over the range T_g to T_g + 90 ºC (see Supporting Information Figure S5 for a VFT fit). First, Equation 14 has no freely adjustable fit parameters: T_c is prescribed uniquely by Equation 13 (but the data must go to sufficiently high temperatures to obtain the Arrhenius slope; otherwise, $E_{a,u}$ becomes a fit parameter). Second, instead of the highly-discussed Vogel temperature T_o in Equation 2, which implies divergence at this temperature,[9,11,12] the convergence temperature T_c avoids such a quandary.

Another feature of Equation 14 is the ability to fit both the Arrhenius and the non-Arrhenius region with the same expression and numerical constants. The VFT equation fails in this regard (see Supporting Information Figure S5 for an illustration of this) since it bends away from the Arrhenius slope at higher temperatures.

Why is T_g at T_g?

At any temperature, the CRR is composed of *n* CRUs, given by Equation 12 and plotted in Figure 3. The number of CRUs at T_g is consistently about 13 ± 1. The specificity of this *n* is in contrast to intensive efforts over the past few decades to identify both the cooperative unit and their number at T_g.

The fact that $n = 13$ at T_g is interpreted to reflect the fact that each pair is surrounded by approximately 12 nearest neighbors. Although static scattering methods show no order, packing simulations by Tanaka et al. suggest a "hexagonal-close-packed-like" arrangement at T_g.[28] If each pair experiences this condition, the entire material is percolated with $n = 13$ cooperatively rearranging regions and thus undergoes the glass transition. If the cooperatively rearranging unit were defined as the number of polyelectrolyte repeat units, *n* would be 26. Significant insight would be provided by molecular dynamics simulations involving the correct number of pairs.

The "size" of the CRR has been a subject of much discussion and confusion.[29] Adam and Gibbs[9] cast the size as the number of cooperative "monomer segments," represented in Equation 11, here termed "units." When small structural units such as $-CH_3$ are defined[30] as "beads" a universal value of 4-5 for the number of beads at T_g is inferred from heat capacity measurements.[29] Alternatively, a linear dimension ε, or volume V_{CRR} ($= \varepsilon^3$) has been used to characterize the CRR.[14] Using calorimetry, Donth concluded ε^3 was large enough to contain up to several hundred repeat units. With 40 wt% water, PDADMA/PSS has 1.35×10^{21} Pol^+Pol^- pairs cm^{-3} for a volume of 0.74 nm^3 per pair. PVBT/PAMPS has 63 wt% water and 2.01×10^{21} Pol^+Pol^- pairs cm^{-3}, for a volume of 0.50 nm^3 per pair. The respective volumes of the CRR at T_g are therefore 9.6 and 6.5 nm^3 (sizes, ε, 2.1 and 1.9 nm) which are in the range of sizes (1 - 3 nm) calculated by Hempel et al.[31] for a number of small and macromolecular glass formers.

Significant Parameters and "Universal" Constants

The Arrhenius parameter required for Equation 14 contains $E_{a,u}$ and $\omega_{o,A}$. The simulated relaxation curves in Figure 3 show the influence of varying $E_{a,u}$ with constant $\omega_{o,A}$ and vice versa (deviations from Arrhenius are shown in Supporting Information Figure S6)..

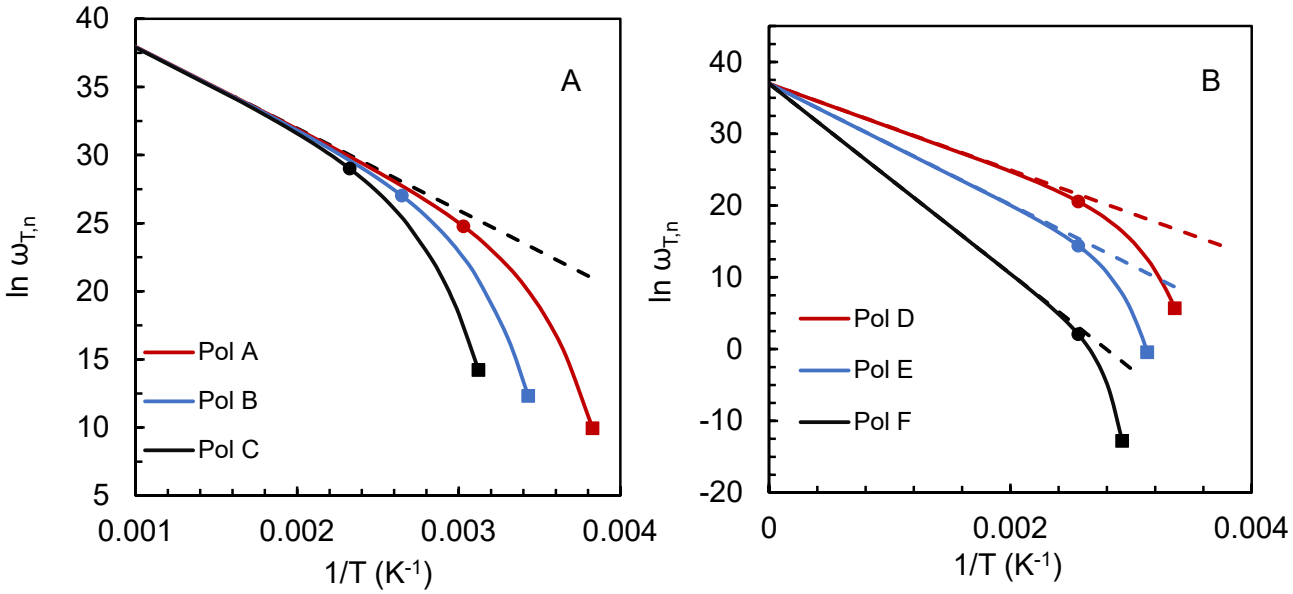

Figure 4. **Simulating the relaxation profile.** Panel **A** simulates the relaxation rate of three polymers with the same $E_{a,u}$ but with different T_c ($E_{a,u}$ = 25.0 kJ mol^{-1},T_c = 330 K, 380 K, 430 K for Pol A, B, C respectively). Panel **B** simulates the relaxation rate of another three polymers with the same T_c but different $E_{a,u}$ (T_c = 390 K; $E_{a,u}$ = 25.0 kJ mol^{-1} , 35.0 kJ mol^{-1}, 55.0 kJ mol^{-1} for D, E, F respectively) T_c and T_g are denoted by the filled circles and squares respectively.

Two parameters in the VFT Equation describe how rapidly the relaxation rate deviates from Arrhenius approaching T_g. The D term in the VFT Equation is known as the "strength parameter." The ratio T_c/T_g tracks D (see Table 1). Alternatively, the "fragility" of a glass

former describes the speed with which the relaxation rate changes at T_g.[32] Assuming *n* is 13 at T_g, the fragility parameter (steepness index), *m*, is given by

$$m = \frac{13E_{a,u}}{2.3RT_g} \quad [15]$$

The *m* values from Equation 14 and from the VFT fits are compared in Table 1.

The analysis of the dynamics of numerous polymers using the WLF equation (Equation 3) has led to the (somewhat controversial) conclusion that the coefficients c_1 and c_2 have "approximately universal" respective values of 10-15 and 50-60 K when the reference temperature is T_g.[9,33] Interestingly, Equation 14 does not specify T_g. Using Equations 11 and 14, the following connection between T_g and T_c may be established:

$$\frac{1}{T_c} = \frac{1}{T_g} - \frac{Rln(n_{Tg}-2)}{E_{a,u}} \quad [16]$$

Assuming $n_{Tg} \approx 13$, Equation 16 may be rearranged to yield a "universal" constant, *U,* of about 20 J mol^{-1} K^{-1} (about 2.4*k,* i.e. about *ek*):

$$U = E_{a,u}\left(\frac{1}{T_g} - \frac{1}{T_c}\right) = Rln(11) \approx 20 \quad [17]$$

Calculated values of *U* are included in Table 1. Frequency shift factors a_T for TTS between temperatures T_1 and T_2 would be given by

$$lna_T = ln\omega_{T1} - ln\omega_{T2} = (n_2 - n_1) + \frac{2E_{a,u}}{R}\left(\frac{1}{T_2} - \frac{1}{T_1}\right) \quad [18]$$

Conclusions

Equation 14 contains no prediction that dynamics should cease at any temperature above 0 K. Although the glass transition depends on the scan or deformation rate and is not itself a thermodynamic phase transition, underlying thermodynamic phenomena are often invoked.[28,34,35] Here, the small change in ion diffusion rate seen near T_g in Figure 2A is an example of a second order transition. According to the mechanism in Scheme 1 this relaxation

mode remains fast and is not cooperative. The small decrease in $E_{a,u}$ from 25.6 kJ mol^{-1} above T_g to 27.1 kJ mol^{-1} below T_g could indicate a transition from a more disordered to a less disordered system ("medium range crystalline order"[28]) on falling through T_g, which would be consistent with a free volume transition.

The intercept $\omega_{o,A}$ (Table 1) for the PECs corresponds to an attempt frequency of about 10^{13} s^{-1}. The physical mechanism summarized by Scheme 1 relates directly to the PEC MCRU (pair exchange) shown in Scheme 2. The identity of the MCRU, though mechanistically a place exchange of a pair of "units," is not as clear for the neutral polymers as it is for the PECs. An attempt frequency of 10^{19} s^{-1} is faster than even the fastest vibrational mode from the lightest/smallest components, whereas the "unit" may be close to a persistence length segment of polymer. Thus, the intercept must be inversely related to the MCRU size. If there are 13 units in the CRR at T_g, to find the size of a unit, values of CRR size ε from Hempel et al.[31] should be divided by $\sqrt[3]{13}$. Using 3.0 and 3.2 nm as the respective values of ε for PS and PVA,[31] yields 1.3 and 1.4 nm for the respective unit sizes, which may be compared with experimental persistence lengths of 1.0 nm[36] and 0.7 nm.[37] Using ε = 1.2 nm from poly(n-butylmethacrylate), the unit size would be 0.5 nm, which compares with ~0.5 nm estimated for the persistence length of PiBMA.[38] Further comparisons are needed for a reliable correlation of persistence length and unit size.

Experimental

Materials. Poly(diallyldimethylammonium chloride) (PDADMAC, M_w 200,000 – 250,000 g mol^{-1}, M_w/M_n ~ 2.7), $NaNO_3$, NaN_3, NaCl, and KBr were obtained from Sigma-Aldrich. Poly(styrenesulfonate), sodium salt (PSSNa, M_w 126,700 g mol^{-1} M_w/M_n = 2.5), poly(2-acrylamido-2-methyl-1-propanesulfonate), sodium salt (PAMPS, 800,000 g mol^{-1}), poly(vinylbenzyl trimethylammonium chloride) (PVBT, $M_w \approx$ 100,000 g mol^{-1}, 26.9 wt% in

water), poly(isobutyl methacrylate) (PiBM, $M_w \approx 260{,}000$ g mol^{-1}), polystyrene (PS, M_w = 210,000 g mol^{-1}) and polyvinylacetate (PVA, $M_w \approx 150{,}000$ g mol^{-1}) were obtained from Scientific Polymer Products.

Acetone (99.5%) from VWR was used for polyelectrolyte fractionation. Deuterium oxide (D_2O, Cambridge Isotope Laboratory, 99.9%) was used for NMR measurements. Deionized water (18.2 MΩ cm) was used to prepare all solutions.

Fractionation. PSSNa and PDADMAC with wide molecular weight distribution were fractionated to provide narrow molecular weight material. PDADMAC and PSS were separately dissolved in 500 mL water to yield 0.2 M solutions and acetone was gradually added as a non-solvent until each solution turned cloudy. The solution was centrifuged and the fraction was collected and dried at 120 °C for 18 h. The procedure was repeated to collect sequential fractions with lower molecular weights.

Size Exclusion Chromatography (SEC). SEC was used to find the weight-average molecular weight, M_w, the number-average molecular weight, M_n, and the polydispersity index, M_w/M_n, = Đ, of PDADMAC and PSS. A 10 μm PSS Novema Max Lux (1000 Å) 300 mm x 8 mm column was used for PDADMAC separations . For PSSNa, a 17 μm column (300 mm x 8 mm, Tosoh Biosciences TSK-GEL G5000PW), alongside a 13 μm column (300 mm x 7.8 mm, Tosoh Biosciences TSK-GEL GMPWx) and a TSK guard column were used. Samples with 30 mg mL^{-1} of PSSNa and PDADMAC were dissolved in 0.3 M $NaNO_3$ mobile phase preserved with 200 ppm NaN_3, and the samples were filtered through a 0.2 μm poly(ether sulfone) filters. The injection volume was 50 μL at a flow rate of 1.0 mL min^{-1}. The detectors were a DAWN-EOS multiangle light scattering (MALS) setup and an Optilab refractometer both from Wyatt Technology. The dn/dc for PSS was 0.175 and that for PDADMA was measured to be 0.186 in the mobile phase used. Eight fractions of PSSNa were collected with a M_w range between 470 and 70.6 kg mol^{-1} and a Đ range of 1.02 to 1.13. Similarly, nine fractions of PDADMAC

were collected with a M_w range of 827 to 39.2 kg mol^{-1} and a Đ range of 1.11 to 1.25 (see Supporting Information Figure S7 for examples of SEC).

PEC formation. PECs were precipitated from stoichiometric mixtures of 0.2 M solutions (polymer concentrations with respect to the monomer unit) 0.25 M NaCl. Fractions of PDADMAC and PSS with matching N were used (PDADMAC, M_w = 70.0 kg mol^{-1}, Đ = 1.13; PSS-Na (M_w = 94.8 kg mol^{-1}, Đ = 1.02). The precipitate was separated from the supernate and washed with 100 mL water for 24 h. The washing process was repeated until the conductivity of the washing solution fell below 50 μS cm^{-1}. The PECs were dried at 120 °C for 24 h then ground into fine powder. The powders were stirred for 30 min in 10 mL 0.01 M NaCl and hot-pressed into either an 8 mm diameter pellet for rheology, or a 3 mm diameter, 2-cm long cylinder for conductivity measurements.

^{1}H NMR. The stoichiometries of the PECs were verified by NMR (Supporting Information Figure S8). 100 mg mL^{-1} of the dry PEC was dissolved in 2.5 M KBr in D_2O and ^{1}H NMR spectra were acquired using an Avance 600 MHz NMR (Bruker).

Measuring Resistivity. PDADMA/PSS and PVBT/PAMPS PEC powders were stirred in 0.5 M NaCl for 30 min. The powders were pressed into 3 mm x 2 cm cylinders at 50 ℃ in a steel mold. The PEC cylinder was heated at 60 ℃ in 0.1 M NaCl and slowly allowed to cool back to room temperature. It was stored in 0.1 M NaCl to equilibrate for 24 h. The PEC was press-fit into a 2.9 mm diameter silicone rubber tube and maintained in 0.1 M NaCl. Silver wires were inserted and sealed into the ends of the rubber tubing and two 0.02” silver wires were inserted into the PEC 0.3 cm apart. The setup was sealed with silicone rubber to ensure the sample was isolated. The sealed sample was then immersed into a water bath with a water jacket and was allowed to equilibrate at 60 ℃. A four-probe conductivity arrangement was then used to measure the conductance of the PEC. Pulses of DC current were applied using a

EG&G Princeton Applied Research 362 Potentiostat and the voltage and current were measured using two Keithley 196 digital multimeters.

Viscoelastic Measurements including T_g. The linear viscoelastic responses of the PDADMA/PSS and PVBT/PAMPS complexes in 0.01 M NaCl were measured using a stress controlled DHR-3 rheometer (TA Instruments). The 8 mm PEC disk was transferred to a cylindrical reservoir and compressed using 8 mm parallel plate geometry until an axial force was recorded. The reservoir was filled with 0.01 M NaCl and capped to prevent solvent evaporation. An axial force of 0.2 N was applied. Frequency sweeps were performed over a temperature range between 0 and 95 °C. The measurements were taken starting from the highest temperature to allow the complex to thermally equilibrate. The PEC was allowed to reach the target temperature by applying a ten-minute delay before each frequency sweep.

For neutral polymers, a 20 mm x 0.1 mm disk was hot pressed. The temperature was regulated between 45 and 350 °C using an TA Instruments ETC oven. The chamber was purged with N_2. The storage and loss modulus of the neutral polymers were recorded over a wide temperature range starting with $T \sim T_g + 250$ and going as low as T_g. Time-temperature superposition was performed using shift factors using T_g as the reference temperature according to Equation 3, shift factors given in Supporting Information Figure S4.

The T_g s were measured using dynamic mechanical analysis (rheometer) with the environment controlled as above. For PDADMA/PSS tanδ (= G''/G') was measured from 10 to 50 °C with a ramp rate of 2 °C min^{-1} under constant strain at eight frequencies between 0.01 and 2 rad s^{-1}. For PVBT/PAMPS and the three neutral polymers, a temperature ramp experiment was carried out at 0.62 rad s^{-1} with a ramp rate of 2 °C min^{-1}. The strain % was held constant throughout the experiment and forward and a backward temperature sweeps were recorded starting from the highest temperature. The forward and backward scans were

averaged and the temperature where the maximum at tanδ (= G''/G') occurs was recorded as T_g.

Acknowledgements

This work was supported by grant DMR1809304 from the National Science Foundation.

Author Contributions

KA performed the experiments. KA and JBS wrote the paper.

Competing Interests statement

No competing interests.

References

1 Debenedetti, P. G. & Stillinger, F. H. Supercooled liquids and the glass transition. *Nature* **410**, 259-267 (2001).
2 Cangialosi, D. Dynamics and thermodynamics of polymer glasses. *Journal of Physics: Condensed Matter* **26**, 153101 (2014).
3 Anderson, P. W. Through the glass lightly. *Science* **267**, 1615-1616 (1995).
4 McKenna, G. B. & Simon, S. L. 50th anniversary perspective: Challenges in the dynamics and kinetics of glass-forming polymers. *Macromolecules* **50**, 6333-6361 (2017).
5 Vogel, H. Das temperaturabhängigkeitsgesetz der viskosität von flussigkeitern. *Phys. Zeit* **22**, 645-646 (1921).
6 Fulcher, G. S. Analysis of recent measurements of the viscosity of glasses. *Journal of the American Ceramic Society* **8**, 339-355 (1925).
7 Tammann, G. Glasses as supercooled liquids. *J. Soc. Glass Technol.* **9**, 166-185 (1925).
8 Williams, M. L., Landel, R. F. & Ferry, J. D. The temperature dependence of relaxation mechanisms in amorphous polymers and other glass-forming liquids. *Journal of the American Chemical Society* **77**, 3701-3707 (1955).
9 Adam, G. & Gibbs, J. H. On temperature dependence of cooperative relaxation properties in glass-forming liquids. *J Chem Phys* **43**, 139-146 (1965).
10 Edwards, S. F. Theory of glasses. *Polymer* **17**, 933-937 (1976).
11 Hecksher, T., Nielsen, A. I., Olsen, N. B. & Dyre, J. C. Little evidence for dynamic divergences in ultraviscous molecular liquids. *Nat Phys* **4**, 737-741 (2008).
12 Lubchenko, V. & Wolynes, P. G. Theory of structural glasses and supercooled liquids. *Annual Review of Physical Chemistry* **58**, 235-266 (2007).
13 Zhao, J., Simon, S. L. & McKenna, G. B. Using 20-million-year-old amber to test the super-arrhenius behaviour of glass-forming systems. *Nat Commun* **4**, 1783 (2013).

14 Berthier, L. *et al.* Direct experimental evidence of a growing length scale accompanying the glass transition. *Science* **310**, 1797-1800 (2005).
15 Akkaoui, K., Yang, M., Digby, Z. A. & Schlenoff, J. B. Ultraviscosity in entangled polyelectrolyte complexes and coacervates. *Macromolecules* **53**, 4234-4246 (2020).
16 Gucht, J. v. d., Spruijt, E., Lemmers, M. & Cohen Stuart, M. A. Polyelectrolyte complexes: Bulk phases and colloidal systems. *Journal of Colloid and Interface Science* **361**, 407-422 (2011).
17 Ghostine, R. A., Shamoun, R. F. & Schlenoff, J. B. Doping and diffusion in an extruded saloplastic polyelectrolyte complex. *Macromolecules* **46**, 4089-4094 (2013).
18 Shaheen, S. A., Yang, M., Chen, B. & Schlenoff, J. B. Water and ion transport through the glass transition in polyelectrolyte complexes. *Chemistry of Materials* **32**, 5994-6002 (2020).
19 Rubinstein, M. & Semenov, A. N. Dynamics of entangled solutions of associating polymers. *Macromolecules* **34**, 1058-1068 (2001).
20 Yang, M., Shi, J. & Schlenoff, J. B. Control of dynamics in polyelectrolyte complexes by temperature and salt. *Macromolecules* **52**, 1930-1941 (2019).
21 Dudowicz, J., Freed, K. F. & Douglas, J. F. Entropy theory of polymer glass formation revisited. I. General formulation. *The Journal of Chemical Physics* **124**, 064901 (2006).
22 Solunov, C. A. Cooperative molecular dynamics and strong/fragile behavior of polymers. *Eur Polym J* **35**, 1543-1556 (1999).
23 Schönhals, A., Kremer, F., Hofmann, A., Fischer, E. W. & Schlosser, E. Anomalies in the scaling of the dielectric alpha-relaxation. *Physical Review Letters* **70**, 3459-3462 (1993).
24 Xu, W.-S., Douglas, J. F. & Freed, K. F. Influence of cohesive energy on relaxation in a model glass-forming polymer melt. *Macromolecules* **49**, 8355-8370 (2016).
25 Freed, K. F. The descent into glass formation in polymer fluids. *Accounts of Chemical Research* **44**, 194-203 (2011).
26 Stickel, F., Fischer, E. W. & Richert, R. Dynamics of glass-forming liquids. I. Temperature-derivative analysis of dielectric relaxation data. *The Journal of Chemical Physics* **102**, 6251-6257 (1995).
27 Sokolov, A. P. Why the glass transition is still interesting. *Science* **273**, 1675-1676 (1996).
28 Tanaka, H., Kawasaki, T., Shintani, H. & Watanabe, K. Critical-like behaviour of glass-forming liquids. *Nature Materials* **9**, 324-331 (2010).
29 Solunov, H. On measuring the characteristic length of the cooperative molecular dynamics in the glass-forming liquids. *J. Phys.: Conf. Ser.* **1186**, 012008 (2019).
30 Wunderlich, B. Study of the change in specific heat of monomeric and polymeric glasses during the glass transition. *The Journal of Physical Chemistry* **64**, 1052-1056 (1960).
31 Hempel, E., Hempel, G., Hensel, A., Schick, C. & Donth, E. Characteristic length of dynamic glass transition near Tg for a wide assortment of glass-forming substances. *Journal of Physical Chemistry B* **104**, 2460-2466 (2000).
32 Martinez, L. M. & Angell, C. A. A thermodynamic connection to the fragility of glass-forming liquids. *Nature* **410**, 663-667 (2001).
33 Hiemenz, P. C. & Lodge, T. *Polymer chemistry*. 2nd edn, (CRC Press, 2007).
34 Hedges, L. O., Jack, R. L., Garrahan, J. P. & Chandler, D. Dynamic order-disorder in atomistic models of structural glass formers. *Science* **323**, 1309-1313 (2009).

35 Stillinger, F. H. & Debenedetti, P. G. Glass transition thermodynamics and kinetics. *Annual Review of Condensed Matter Physics* **4**, 263-285 (2013).

36 Wignall, G. D., Ballard, D. G. H. & Schelten, J. Measurements of persistence length and temperature dependence of the radius of gyration in bulk atactic polystyrene. *Eur Polym J* **10**, 861-865 (1974).

37 Tyagi, M., Arbe, A., Alegría, A., Colmenero, J. & Frick, B. Dynamic confinement effects in polymer blends. A quasielastic neutron scattering study of the slow component in the blend poly(vinyl acetate)/poly(ethylene oxide). *Macromolecules* **40**, 4568-4577 (2007).

38 Geng, K. *et al.* Conflicting confinement effects on the Tg, diffusivity, and effective viscosity of polymer films: A case study with poly(isobutyl methacrylate) on silica and possible resolution. *Macromolecules* **50**, 609-617 (2017).

Table of Contents Graphic